



Onset of drying and dormancy in relation to water dynamics of semi-arid grasslands from MODIS NDWI

Chao Ding^a, Xiangnan Liu^{a,*}, Fang Huang^b, Yao Li^c, Xinyu Zou^a

^a School of Information Engineering, China University of Geosciences, Beijing 100083, China

^b School of Geographical Sciences, Northeast Normal University, Changchun 130024, China

^c Institute of Remote Sensing and Digital Earth, Chinese Academy of Sciences, Beijing 100101, China

ARTICLE INFO

Article history:

Received 14 June 2016

Received in revised form

28 November 2016

Accepted 10 December 2016

Available online 15 December 2016

Keywords:

Autumn phenology

Climate variability

Remote sensing

MODIS time series

NDWI

Songnen plain

Grasslands

ABSTRACT

Our knowledge of autumn phenology and its response to climate variability is currently limited. One way to improve our understanding of autumn phenology at the landscape scale is to investigate autumn vegetation dynamics based on multiple vegetation indices from remote sensing data. In this study, we derived two autumn phenological metrics (phenometrics), onset of drying and dormancy, for semi-arid grasslands from MODIS normalized difference water index (NDWI) time series. The onset of drying represents the start of decline in the vegetation's metabolism during autumn, and the onset of NDWI-based dormancy signifies the end of metabolic activity. These NDWI-based phenometrics were then compared with enhanced vegetation index (EVI)-based phenometrics in northeastern China from 2001 to 2013. Influences of climatic variability on autumn phenology were analyzed using partial correlation analysis. We found that, in general, the onset of drying was slightly later than the onset of EVI-based senescence. Both did not strongly correlate with precipitation and mean minimum temperature in August. The onset of NDWI-based dormancy had, on average, a time lag of seven days, relative to the onset of EVI-based dormancy during 2001–2013. Moreover, it showed a much stronger response to mean minimum temperature in September than EVI-based dormancy. A colder autumn generally advanced the onset of NDWI-based dormancy, while it had little effect on the onset of EVI-based dormancy in the study area. These results suggest that phenological studies using NDWI could expand our understanding of land surface phenology. Furthermore, considering the different responses of the onset of NDWI- and EVI-based dormancy to climate variability, a combination of these phenometrics could contribute to the study of the ecosystem processes (e.g., carbon cycle) in semi-arid grasslands.

© 2016 Elsevier B.V. All rights reserved.

1. Introduction

Phenology plays an important role in studying global change because phenological variability reflects the ecological response to climate variability, and affects the feedback of vegetation to the climate system (Penuelas et al., 2009; Richardson et al., 2013a; Schwartz, 1999; Walther et al., 2002). To date, the influence of environmental factors (e.g., temperature and precipitation) on spring phenology is better understood than that on autumn phenology (Dragoni and Rahman, 2012; Richardson et al., 2013a; Yang et al.,

2014b). More attention needs to be paid to autumn phenology and its response to climate variability (Gallinat et al., 2015; Richardson et al., 2013a). Expanding observations of autumn phenology at different scales (e.g., species and landscape scales) is critical to improve our understanding of it (Gallinat et al., 2015; Garrity et al., 2011).

Satellite remote sensing serves as a powerful technique for detecting vegetation phenology (Justice et al., 1985; Reed et al., 1994; White et al., 1997). Vegetation phenology observed from satellite remote sensing is termed land surface phenology, which characterizes the seasonality of vegetation at the landscape scale (Friedl et al., 2006; Henebry, 2003). Remote sensing of autumn phenology typically focuses on deriving the onset of vegetation senescence, dormancy, or the end of growing season from vegetation indices time series (e.g., Dragoni et al., 2011; Ganguly et al., 2010; Gonsamo and Chen, 2016; Zhang and Goldberg, 2011).

* Corresponding author at: School of Information Engineering, China University of Geosciences, Beijing 100083, China.

E-mail addresses: dc@cugb.edu.cn (C. Ding), liuxn@cugb.edu.cn (X. Liu), huangf835@nenu.edu.cn (F. Huang).

The normalized difference vegetation index (NDVI) and enhanced vegetation index (EVI) are the two most commonly used vegetation indices for autumn phenological studies (e.g., de Beurs and Henebry, 2010a; Garonna et al., 2014; Liu et al., 2015; Jeong et al., 2011; Zhang et al., 2012). However, using only greenness vegetation indices cannot comprehensively characterize autumn vegetation dynamics because vegetation senescence is accompanied by various biophysical and biochemical dynamics, for instance, changes in pigment content, water content, leaf area index, and canopy roughness. To expand our knowledge of vegetation dynamics in autumn at the landscape scale, it is essential to investigate autumn phenology derived from alternative vegetation indices or parameters (Henebry and de Beurs, 2013).

Satellite observations at longer wavelengths, for example from short-wave infrared or microwaves, could assist in better describing phenological changes related to the vegetation water content. In microwave region, vegetation optical depth, which is sensitive to biomass and water content, derived from the Advanced Microwave Scanning Radiometer for Earth Observation System (AMSR-E) has been used to monitor land surface phenology (e.g., Guan et al., 2014; Jones et al., 2011). Vegetation optical depth and NDVI were found to provide distinctive land surface phenology in several ecosystems (Guan et al., 2014; Jones et al., 2011). In short-wave infrared region, the potential of vegetation water indices, for instance, the normalized difference water index (NDWI, Gao, 1996), for tracking vegetation dynamics has been demonstrated in several ecosystems (e.g., Boles et al., 2004; de Beurs et al., 2009; de Beurs and Henebry, 2010b; Delbart et al., 2005; Xiao et al., 2002). However, efforts to detect phenology using vegetation water indices are still limited. They were commonly used as an alternative solution to reduce the influence of snow cover in boreal regions (Delbart et al., 2005, 2006; Thompson et al., 2015). The capabilities of vegetation water indices for characterizing vegetation dynamics may be under-utilized for some ecosystems (Wu et al., 2014). As water content is a sensitive indicator of the strength of plant metabolism (e.g., photosynthesis, respiration, and transpiration), vegetation water indices time series could provide new insight in land surface phenology.

The aims of this study are (1) to define two autumn phenological metrics (phenometrics) in semi-arid grasslands, onset of drying and dormancy, from MODIS NDWI time series, (2) to compare the NDWI- and EVI-based autumn phenometrics, and (3) to evaluate the sensitivity of these phenometrics to climate variability.

2. Materials and methods

2.1. Study area

The study area is situated in the Songnen Plain in northeastern China (Fig. 1). The mean altitude is about 150 m. This area has a semi-arid continental monsoon climate. The mean annual temperature ranges from 4.3 to 6.7 °C. The mean annual precipitation ranges from 300 to 460 mm, and most of the precipitation occurs from June to August. The area is snow-covered during late October to early April. The predominant land cover types are grasslands and croplands (Fig. 1(b)). The spatial distribution of grasslands in this area was obtained from the MODIS land cover type product (MCD12Q1). This product provides annual land cover type at a 500 m spatial resolution based on five land cover type classification schemes (Friedl et al., 2010). The MCD12Q1 data from 2001 to 2013, using the International Geosphere Biosphere Programme (IGBP) classification scheme, were selected. To reduce the influence of land cover change on the analysis of variability in land surface phenology, only grasslands that were consistently classified as such for all 13 years were retained.

2.2. MODIS surface reflectance product

We selected the MODIS MOD09A1 product, which provides 8-day composite surface reflectance data with a spatial resolution of 500 m, to obtain the NDWI and EVI time series. The effects of atmospheric gases and aerosols are corrected in this product. For each 8-day period, observations with the highest quality are selected based on cloud state, aerosol quantity, observation coverage, and view angle (Vermette et al., 2011). All available Terra MOD09A1 data for the study area (MODIS tile number: h26v04) from January 1, 2001 to December 31, 2013 were used. NDWI and EVI were calculated as follows:

$$NDWI = \frac{\rho_{b2} - \rho_{b6}}{\rho_{b2} + \rho_{b6}} \quad (1)$$

$$EVI = 2.5 \times \frac{\rho_{b2} - \rho_{b1}}{\rho_{b2} + 6 \times \rho_{b1} - 7.5 \times \rho_{b3} + 1} \quad (2)$$

where ρ_{b1} , ρ_{b2} , ρ_{b3} , and ρ_{b6} are the reflectance of band 1 (620–670 nm), band 2 (841–876 nm), band 3 (459–479 nm), and band 6 (1628–1652 nm) of MODIS, respectively. MODIS also contains another two water absorption bands: band 5 (1230–1250 nm) and 7 (2105–2155 nm). However, images of band 5 have obvious

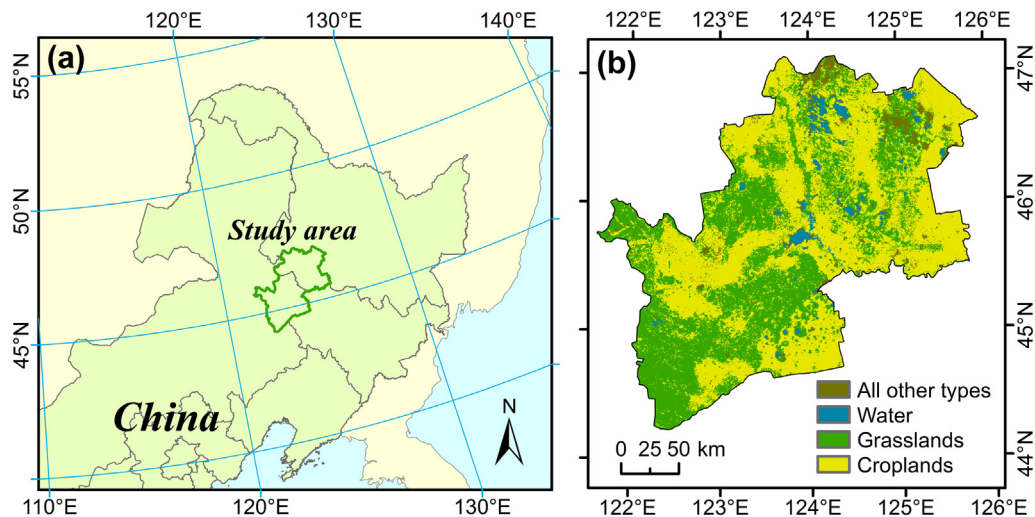


Fig. 1. Overview of the study area. (a) Location of the study area. (b) The land cover types in 2013 provided by the MODIS MCD12Q1 product.

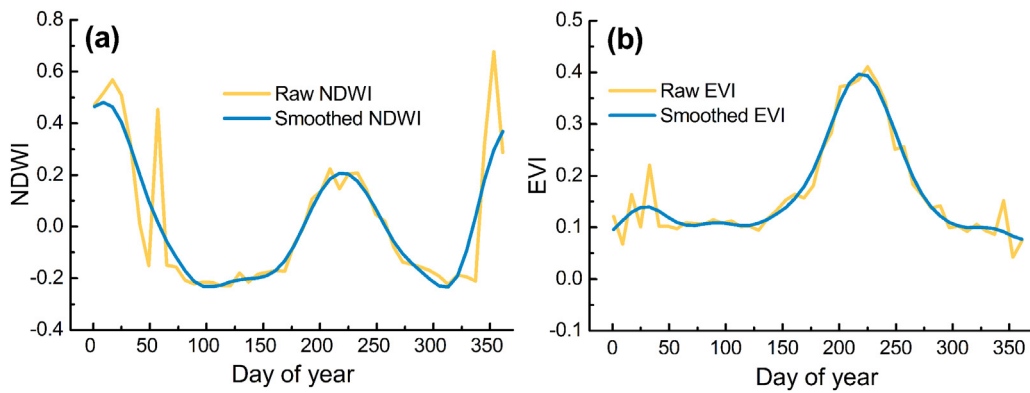


Fig. 2. The raw and smoothed NDWI and EVI time series for the same pixel in 2013.

striping, which hinders its application for phenological studies. Band 6 was selected in this study because a spectral band near 1640 nm is also available for SPOT VEGETATION and Landsat data; hence, NDWI using this spectral band from these different data sources could be comparable. We note that in various studies NDWI is also referred to as normalized difference infrared index (NDII, Gonsamo et al., 2012; Thompson et al., 2015; Townsend et al., 2012) and land surface water index (LSWI, Jin et al., 2013; Xiao et al., 2009).

2.3. Gridded meteorological data

Monthly mean minimum temperature and accumulated precipitation for 2001–2013, at 0.5° spatial resolution, were obtained from the National Meteorological Information Center of China (<http://data.cma.cn/>). These gridded data sets were produced through thin plate spline interpolation by using the meteorological data from 2472 national meteorological stations across China and the GTOPO30 digital elevation model (DEM) data. We resampled the gridded data to a 500 m spatial resolution to match the MODIS data for further analysis.

2.4. Detection of autumn phenology

Model fitting (e.g., Beck et al., 2006; Elmore et al., 2012; Klosterman et al., 2014; Zhang et al., 2003) and smoothing-interpolation (e.g., Keenan et al., 2014; Piao et al., 2006) are widely

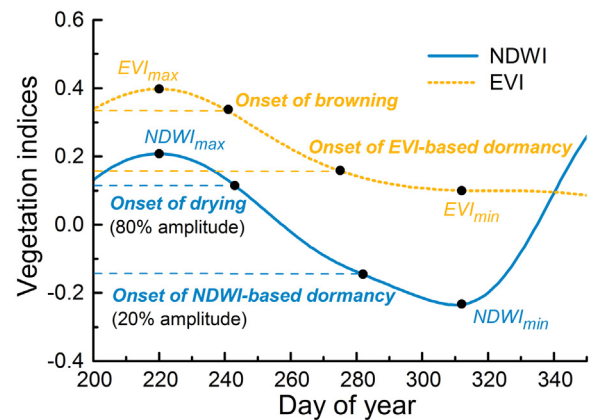


Fig. 3. Example of detecting autumn phenology from NDWI and EVI time series for the same pixel in 2013.

used methods for modeling vegetation indices time series. Considering the complexity of natural vegetation dynamics and the relatively short autumn decay process of grasslands in the study area, the smoothing-interpolation method was adopted for modeling NDWI and EVI time series. We first used the quality flags in the MOD09A1 product to reduce the noise of cloud and cloud shadow. If the state of a point in the time series was identified as cloud or cloud shadow, its corresponding vegetation index value was lin-

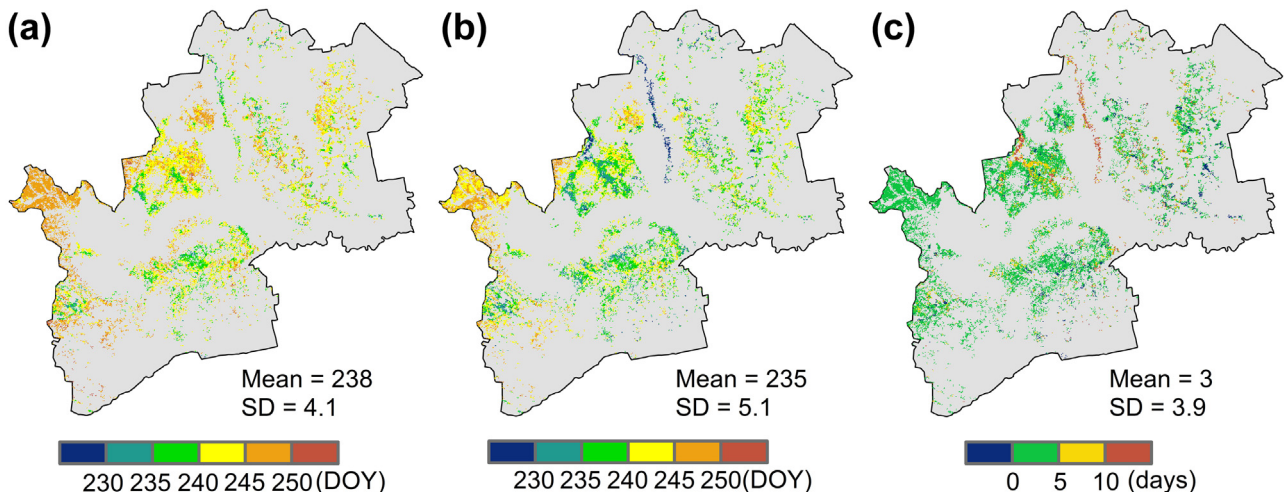


Fig. 4. Spatial distributions of the mean date of (a) the onset of drying and (b) browning during 2001–2013. (c) Difference between (a) and (b). SD in the figure represents standard deviation.

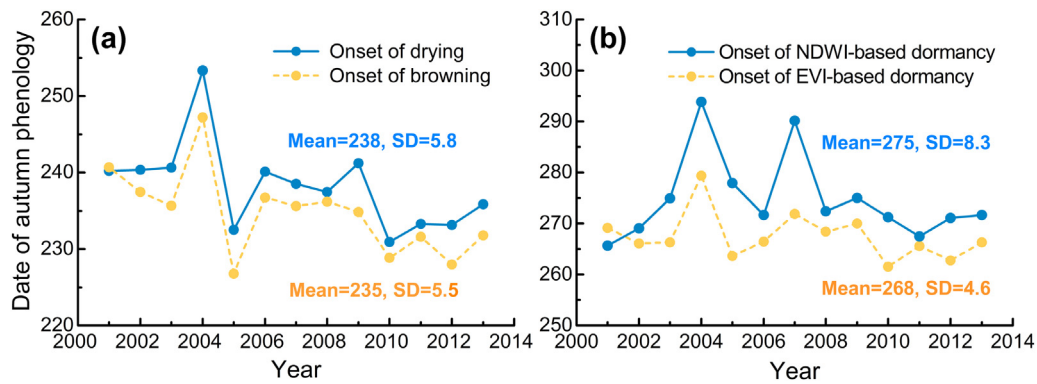


Fig. 5. Interannual variabilities in (a) the onset of drying and browning, (b) the onset of NDWI- and EVI-based dormancy over the entire study area.

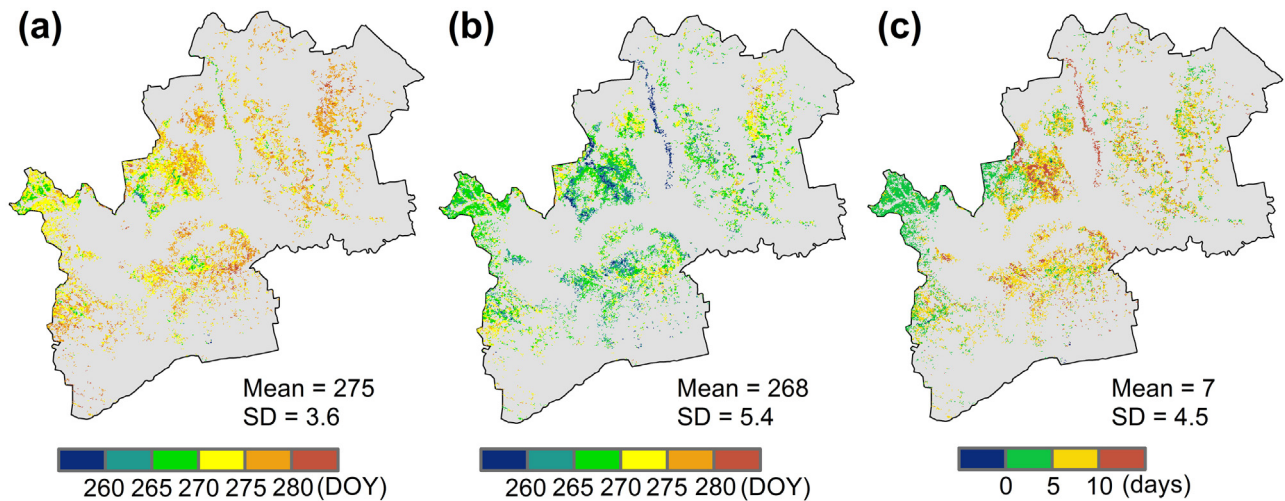


Fig. 6. Spatial distributions of the mean date of (a) the onset of NDWI-based dormancy and (b) EVI-based dormancy during 2001–2013. (c) Difference between (a) and (b).

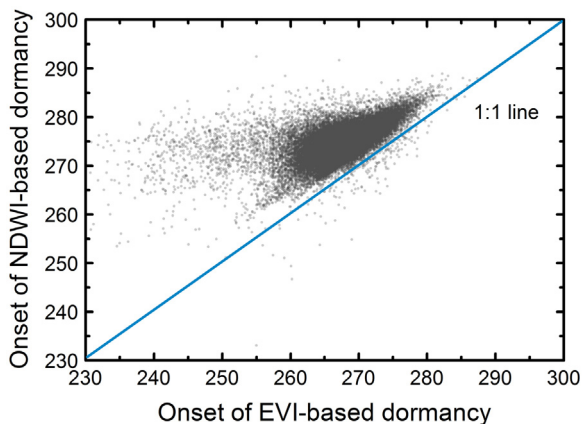


Fig. 7. Relationship between the mean dates of the onset of NDWI- and EVI-based dormancy during 2001–2013.

early interpolated using the values of the two most recent clear points. The time series were then smoothed using the stationary wavelet transform, which has been shown to work well for reducing noise in MODIS NDVI time series (Lu et al., 2007). We decomposed the vegetation index time series into one low-frequency signal and three high-frequency signals, with a mother wavelet function of Daubechies 3 and a decomposition level of three. The two high-

est frequency signals were regarded as noise and were excluded in the reconstruction of the time series. An example of the smoothed NDWI and EVI time series is provided in Fig. 2.

The subsequent analyses only focused on the autumn decay processes in the NDWI and EVI time series. The minimum point ($NDWI_{min}$, Fig. 3) between day of year (DOY) 274 (early October) and DOY 321 (Mid-November), and the maximum point ($NDWI_{max}$) between DOY 121 (early May) and the date of $NDWI_{min}$ were used to determine the start and end of the decay process of the NDWI time series. The date of $NDWI_{min}$ was also used as the autumn minimum point of the EVI time series (EVI_{min}) to reduce the influence of snow cover on EVI. Seasonal maximum of EVI was determined between DOY 121 and the date of EVI_{min} . Finally, we used the cubic spline interpolation to generate daily NDWI and EVI time series.

Two key autumn phenometrics were analyzed in this study: onset of senescence and dormancy. The onset of senescence was defined as the date corresponding to an 80% amplitude in the autumn decay process of the modeled vegetation index time series. Summer drought stress may result in multiple 80% amplitude points; in this case, the last one was identified as the onset of senescence. For the onset of dormancy, a 20% amplitude was used. The onset of EVI-based senescence is hereafter known as the onset of browning because, in terms of greenness, browning is a visible phenomenon of senescence for grasslands. For NDWI-based autumn phenometrics, the onset of senescence is hereafter known as the onset of drying.

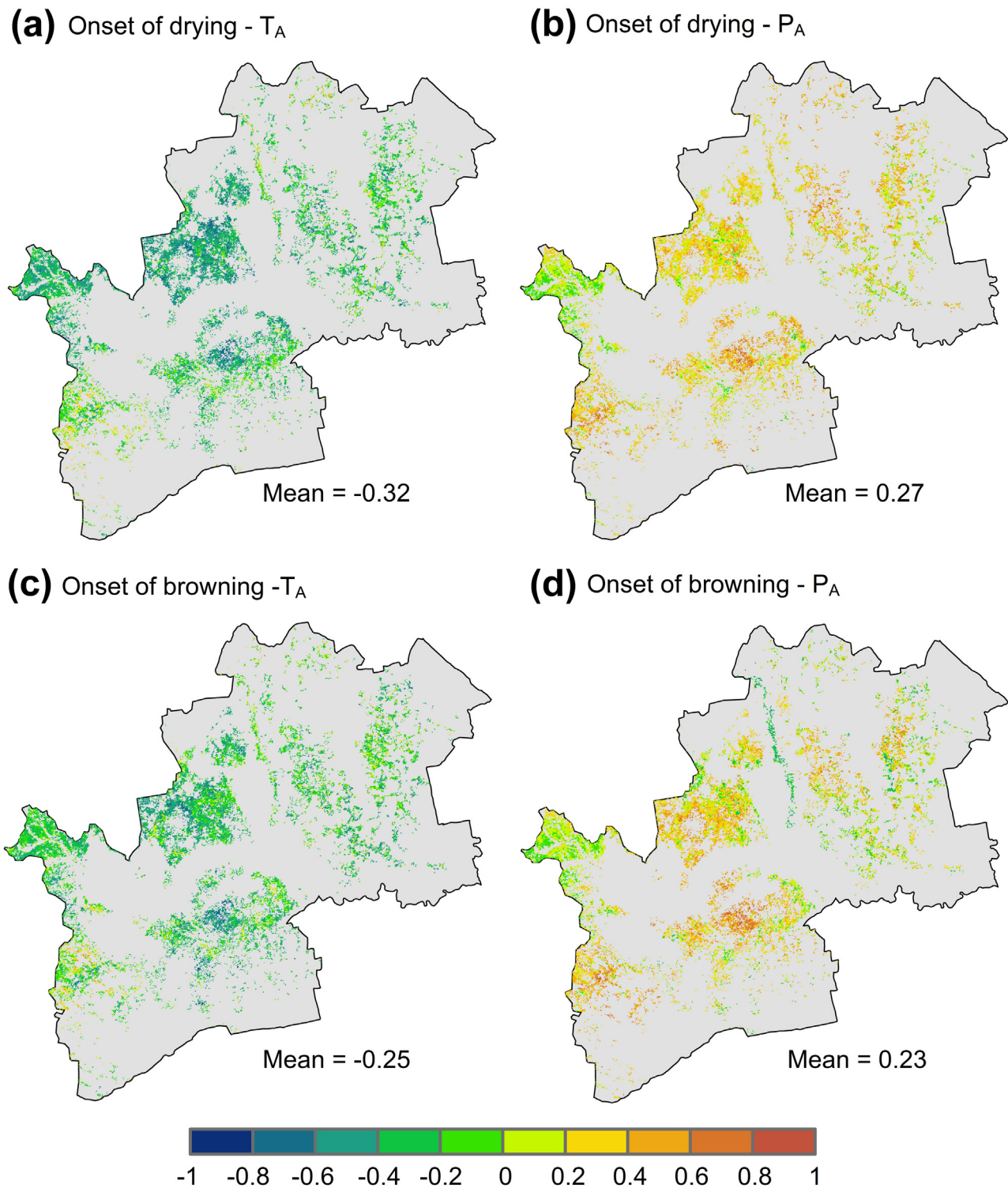


Fig. 8. Partial correlation coefficients between the onset of senescence and climatic factors. (a) The onset of drying and mean minimum temperature in August (T_A). (b) The onset of drying and precipitation in August (P_A). (c) The onset of browning and T_A . (d) The onset of browning and P_A .

2.5. Analyzing the influence of climate variability on autumn phenology

The relationship between autumn phenology and climatic factors was examined using a partial correlation analysis, which computes the correlation between two variables, with the effects of other related variables removed. Because the onset of drying and

browning generally occurred in late August during 2001–2013 for the study area (provided in Section 3.1), partial correlation coefficients (R) between climatic factors, including mean minimum temperature (T_A) and precipitation (P_A) in August, and the onset of drying and browning were calculated. The onset of NDWI- and EVI-based dormancy generally occurred in late September and early October, therefore, we analyzed the influence of mean minimum

temperature (T_S) and precipitation (P_S) in September on the onset of NDWI- and EVI-based dormancy. Minimum temperature was used because it is generally a limiting factor of vegetation activity in autumn and has been used to predict autumn vegetation senescence (Jolly et al., 2005).

3. Results

3.1. Comparison of NDWI- and EVI-based autumn phenology

Generally, the onset of drying was slightly later than the onset of browning. For the mean date of the onset of drying and browning during 2001–2013, 91% of the pixels in the study area showed a later date of the onset of drying (Fig. 4(c)). The spatial mean date of the onset of drying was consistently later than that of the onset of browning, except for 2001 (Fig. 5(a)). The spatial-temporal mean time lag of the onset of drying relative to the onset of browning was three days.

The onset of NDWI-based dormancy was also generally later than the onset of EVI-based dormancy. In the study area, 98% of the pixels had a later mean date of the onset of NDWI-based dormancy during 2001–2013 (Figs. 6(c), 7). Regarding the spatial mean date of the onset of dormancy, a later onset of NDWI-based dormancy was also observed every year, with the exception of 2001. The spatial-temporal mean time lag was seven days. Furthermore, the onset of NDWI-based dormancy showed a greater interannual variability (SD 8.3 days) than that of EVI-based dormancy (SD 4.6 days, Fig. 5(b)).

3.2. Influence of climate variability on autumn phenology

The onset of drying negatively correlated with T_A , and had a mean partial correlation coefficient (R_{mean}) of -0.32 (Fig. 8(a)). A statistically significant correlation ($p < 0.05$) was found for 10% of the total pixels in the study area. Correlations between the onset of drying and P_A were generally positive (Fig. 8(b)) with an R_{mean} of 0.27. Percentage of significant correlation was 7%.

The onset of browning also showed a negative correlation with T_A and had an R_{mean} of -0.25 (Fig. 8(c)). Six percent of the pixels showed significant correlation. A positive correlation between the onset of browning and P_A was observed. The R_{mean} was 0.23, and the correlation was significant for 8% of the pixels (Fig. 8(d)). In general, neither the onset of drying nor the onset of browning showed strong responses to T_A and P_A in the study area.

The onset of NDWI-based dormancy positively correlated with T_S and had an R_{mean} of 0.43 (Fig. 9(a)). There was a significant correlation for 30% of the pixels. Colder autumn generally advanced the onset of NDWI-based dormancy in this area. In contrast, P_S did not show strong control on the onset of NDWI-based dormancy onset with an R_{mean} of -0.11 (Fig. 9(b)).

An unexpectedly weak correlation ($R_{\text{mean}} = 0.09$) between T_S and the onset of EVI-based dormancy was observed (Fig. 9(c)). Only 4% of the pixels had a significant correlation. In addition, 37% of the pixels had a negative R value, even if not statistically significant. Meanwhile, the onset of EVI-based dormancy did not correlate with P_S ($R_{\text{mean}} = -0.09$, Fig. 9(d)). Generally, the onset of EVI-based dormancy was not controlled by T_S and P_S in the study area.

4. Discussion

We found that NDWI-based autumn phenology was generally later than EVI-based autumn phenology. The differences between NDWI- and EVI-based autumn phenology can be attributed to two categories of factors: (1) abiotic factors, particularly soil moisture, and (2) physiological processes. As fractional vegetation cover

is generally less than 100% in these semi-arid grasslands, the strongest influence of soil moisture on NDWI may occur during the wet season (June–August). Therefore, the detection of autumn phenology, especially the onset of drying that occurs close to the wet season, may be most affected. However, the difference between the onset of drying and browning was small. On the other hand, soil moisture in the study area showed strong spatial-temporal heterogeneity due to the spatial-temporal heterogeneity of precipitation. If the differences between the NDWI- and EVI-based autumn phenology were dominated by soil moisture variability, the NDWI-based autumn phenology couldn't consistently later than EVI-based autumn phenology. However, later dates for the NDWI-based autumn phenometrics relative to the EVI-based autumn phenometrics were observed for most pixels across all years, except for 2001. In 2001, the area suffered serious drought, leading to anomalous vegetation dynamics. Despite the effects of drought in 2001, the results indicate that soil moisture was not the dominant factor that induced a later NDWI-based autumn phenology. Nevertheless, to detect vegetation phenology in relation to water dynamics more accurately in regions with low fractional vegetation cover, it is recommended to consider the effects of soil moisture on vegetation water indices, for example, developing vegetation water indices that are insensitive to soil moisture or reducing the effects of soil moisture on NDWI through mixed pixel decomposition.

EVI (or NDVI)-based phenology are generally thought to measure the seasonality of photosynthetic activity (Piao et al., 2006; Reed et al., 2009). As most plant physiological activities are related to plant water content, NDWI-based autumn phenology provides an alternative measure of vegetation status change. The time lag of NDWI-based autumn phenology may be due to a faster decline in photosynthetic activity than any other physiological activity (e.g., respiration) in the decay process of grasslands. Although close to the onset of browning, the onset of drying has a different ecological meaning. It represents the start of the decline in vegetation's metabolism during autumn. The onset of NDWI-based dormancy generally represents the end of the metabolic activity of vegetation.

High temporal resolution ground-based spectral, biochemical, biophysical, and phenological measurements (e.g., Hmimina et al., 2013; Liang et al., 2011; Yang et al., 2014a), CO_2 eddy flux observations (e.g., Garrity et al., 2011; Richardson et al., 2010; Xiao et al., 2009), and near surface remote sensing observations (e.g., Hufkens et al., 2012; Klosterman et al., 2014; Richardson et al., 2013b) can substantially deepen our understanding of the ecological meanings of land surface phenology from multiple vegetation indices. Combinations of multiple vegetation indices for detecting phenology have been suggested in a few recent studies (e.g., Gonsamo et al., 2012; Guan et al., 2014; Thompson et al., 2015; Wu et al., 2014). Clarifying the differences between phenometrics derived from multiple vegetation indices is a logic basis for combining these indices.

For the relationships between autumn phenology and climate factors, a very low mean correlation coefficient between the onset of EVI-based dormancy onset and T_S was found, while the onset of NDWI-based dormancy showed a stronger correlation with T_S . These results suggest that phenological studies using NDWI can provide us with new insight into the relationship between vegetation dynamics and climate variability. Furthermore, exploring the influence of other environmental factors, such as photoperiod, on autumn phenology from multiple vegetation indices in semi-arid grasslands is recommended to better understand the drivers of autumn phenology. A warmer autumn was reported to increase respiratory activity more than photosynthetic activity, leading to an earlier termination of the net carbon uptake period in northern ecosystems (Piao et al., 2008). Considering the different responses of the onset of NDWI- and EVI-based dormancy to autumn temperature, the integration of these phenometrics may contribute to

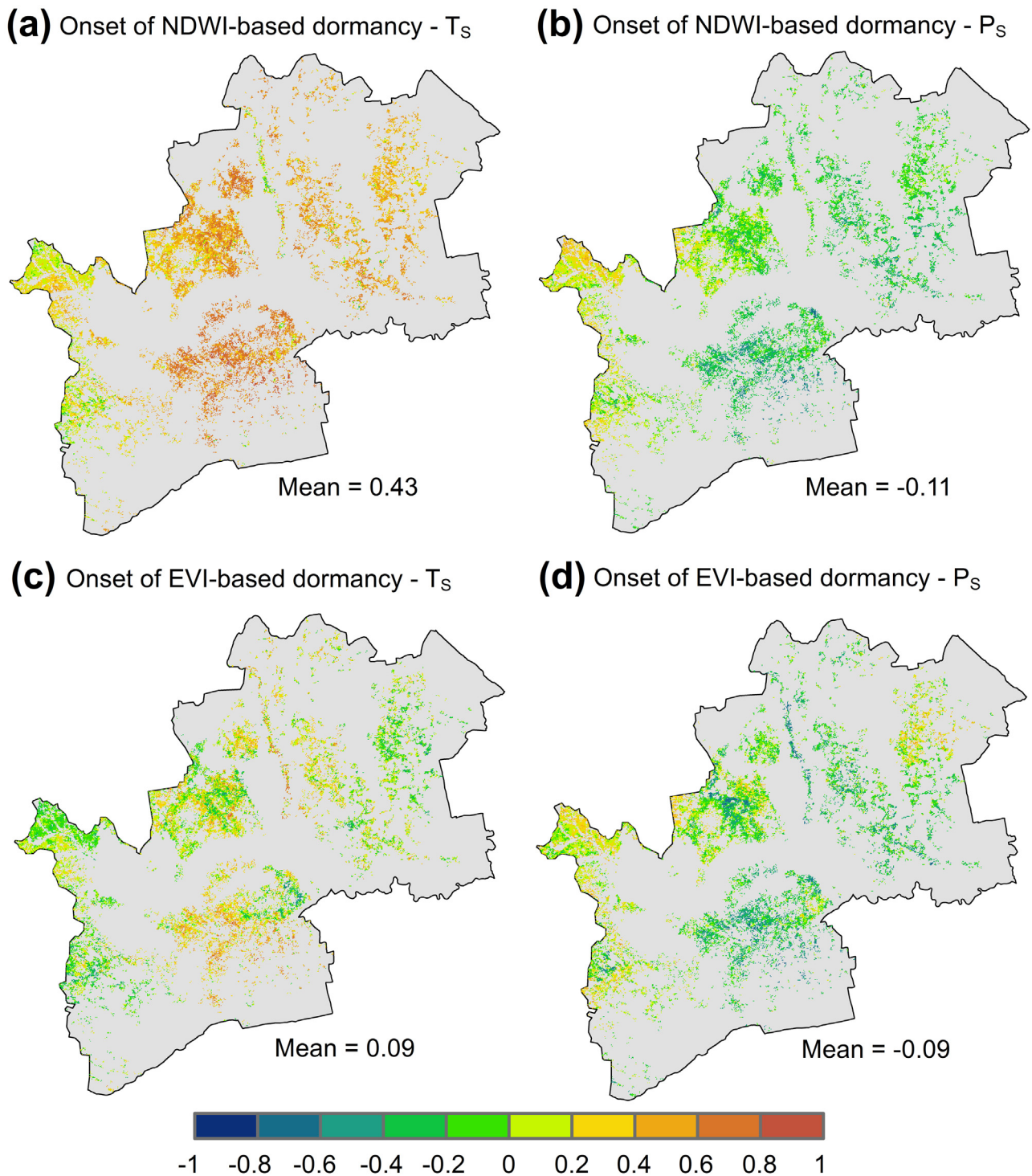


Fig. 9. Partial correlation coefficients between the onset of dormancy and climatic factors. (a) The onset of NDWI-based dormancy and mean minimum temperature in September (T_S). (b) The onset of NDWI-based dormancy and precipitation in September (P_S). (c) The onset of EVI-based dormancy and T_S . (d) The onset of EVI-based dormancy and P_S .

our further understanding of the phenological controls on carbon uptake in semi-arid grasslands.

5. Conclusions

We defined two autumn phenometrics, the onset of drying and dormancy, to describe canopy water dynamics for semi-arid temperate grasslands, by using MODIS NDWI. The onset of drying is

an indicator of the start of senescence, representing a decline in vegetation's metabolism in autumn, and the onset of NDWI-based dormancy measures the date that the metabolic activity of vegetation ends.

In general, the onset of drying was slightly later than that of EVI-based browning, while a larger time lag of the onset of NDWI-based dormancy, relative to the onset of EVI-based dormancy, was observed. A colder autumn generally advanced the

onset of NDWI-based dormancy. The onset of NDWI-based dormancy showed the potential to track ecosystem processes (e.g., carbon cycle) in semi-arid grasslands. The differences between NDWI- and EVI-based autumn phenology highlight that combining multiple vegetation indices can help to improve our understanding of vegetation dynamics in the context of global change.

Acknowledgements

This work was supported by the National Natural Science Foundation of China (Grant No. 41571405). The MOD09A1 and MCD12Q1 datasets were acquired from the Level-1 & Atmosphere Archive and Distribution System (LAADS) Distributed Active Archive Center (DAAC), located in the Goddard Space Flight Center in Greenbelt, Maryland (<https://ladsweb.nascom.nasa.gov/>). We are grateful to the two reviewers for their constructive comments.

References

- Beck, P.S.A., Atzberger, C., Hogda, K.A., Johansen, B., Skidmore, A.K., 2006. Improved monitoring of vegetation dynamics at very high latitudes: a new method using MODIS NDVI. *Remote Sens. Environ.* 100 (3), 321–334.
- Boles, S.H., et al., 2004. Land cover characterization of Temperate East Asia using multi-temporal VEGETATION sensor data. *Remote Sens. Environ.* 90 (4), 477–489.
- de Beurs, K.M., Henebry, G.M., 2010a. Spatio-temporal statistical methods for modeling land surface phenology. In: Hudson, I.L., Keatley, M.R. (Eds.), *Phenological Research: Methods for Environmental and Climate Change Analysis*. Springer, Dordrecht.
- de Beurs, K.M., Henebry, G.M., 2010b. A land surface phenology assessment of the northern polar regions using MODIS reflectance time series. *Can. J. Remote Sens.* 36, S87–S110.
- de Beurs, K.M., Wright, C.K., Henebry, G.M., 2009. Dual scale trend analysis for evaluating climatic and anthropogenic effects on the vegetated land surface in Russia and Kazakhstan. *Environ. Res. Lett.* 4 (4).
- Delbart, N., Kergoat, L., Le Toan, T., Lhermitte, J., Picard, G., 2005. Determination of phenological dates in boreal regions using normalized difference water index. *Remote Sens. Environ.* 97 (1), 26–38.
- Delbart, N., Le Toan, T., Kergoat, L., Fedotova, V., 2006. Remote sensing of spring phenology in boreal regions: a free of snow-effect method using NOAA-AVHRR and SPOT-VGT data (1982–2004). *Remote Sens. Environ.* 101, 52–62.
- Dragoni, D., Rahman, A.F., 2012. Trends in fall phenology across the deciduous forests of the Eastern USA. *Agric. Forest Meteorol.* 157, 96–105.
- Dragoni, D., et al., 2011. Evidence of increased net ecosystem productivity associated with a longer vegetated season in a deciduous forest in south-central Indiana, USA. *Glob. Change Biol.* 17 (2), 886–897.
- Elmore, A.J., Guinn, S.M., Minsley, B.J., Richardson, A.D., 2012. Landscape controls on the timing of spring, autumn, and growing season length in mid-Atlantic forests. *Glob. Change Biol.* 18 (2), 656–674.
- Friedl, M., et al., 2006. Land Surface Phenology: A Community White Paper Requested by NASA (April 10). <http://cce.nasa.gov/mtg2008.ab-presentations/Phenology-Friedl.whitepaper.pdf>.
- Friedl, M.A., et al., 2010. MODIS Collection 5 global land cover: algorithm refinements and characterization of new datasets. *Remote Sens. Environ.* 114 (1), 168–182.
- Gallinat, A.S., Primack, R.B., Wagner, D.L., 2015. Autumn, the neglected season in climate change research. *Trends Ecol. Evol.* 30 (3), 169–176.
- Ganguly, S., Friedl, M.A., Tan, B., Zhang, X.Y., Verma, M., 2010. Land surface phenology from MODIS: characterization of the Collection 5 global land cover dynamics product. *Remote Sens. Environ.* 114 (8), 1805–1816.
- Gao, B.C., 1996. NDWI – A normalized difference water index for remote sensing of vegetation liquid water from space. *Remote Sens. Environ.* 58 (3), 257–266.
- Garonna, I., et al., 2014. Strong contribution of autumn phenology to changes in satellite-derived growing season length estimates across Europe (1982–2011). *Glob. Change Biol.* 20 (11), 3457–3470.
- Garrity, S.R., et al., 2011. A comparison of multiple phenology data sources for estimating seasonal transitions in deciduous forest carbon exchange. *Agric. Forest Meteorol.* 151 (12), 1741–1752.
- Gonsamo, A., Chen, J.M., 2016. Circumpolar vegetation dynamics product for global change study. *Remote Sens. Environ.* 182, 13–26.
- Gonsamo, A., Chen, J.M., Price, D.T., Kurz, W.A., Wu, C.Y., 2012. Land surface phenology from optical satellite measurement and CO₂ eddy covariance technique. *J. Geophys. Res.-Biogeosci.*, 117.
- Guan, K.Y., et al., 2014. Terrestrial hydrological controls on land surface phenology of African savannas and woodlands. *J. Geophys. Res.-Biogeosci.* 119 (8), 1652–1669.
- Henebry, G.M., de Beurs, K.M., 2013. Remote sensing of land surface phenology: a prospectus. In: Schwartz, M.D. (Ed.), *Phenology: An Integrative Environmental Science* (second edition). Springer, Dordrecht.
- Henebry, G.M., 2003. *Grasslands of the North American great plains*. In: Schwartz, M.D. (Ed.), *Phenology: An Integrative Environmental Science*. Kluwer, Dordrecht/Boston.
- Hmimina, G., et al., 2013. Evaluation of the potential of MODIS satellite data to predict vegetation phenology in different biomes: an investigation using ground-based NDVI measurements. *Remote Sens. Environ.* 132, 145–158.
- Hufkens, K., et al., 2012. Linking near-surface and satellite remote sensing measurements of deciduous broadleaf forest phenology. *Remote Sens. Environ.* 117, 307–321.
- Jeong, S.J., Ho, C.H., Gim, H.J., Brown, M.E., 2011. Phenology shifts at start vs. end of growing season in temperate vegetation over the Northern Hemisphere for the period 1982–2008. *Glob. Change Biol.* 17 (7), 2385–2399.
- Jin, C., et al., 2013. Phenology and gross primary production of two dominant savanna woodland ecosystems in Southern Africa. *Remote Sens. Environ.* 135, 189–201.
- Jolly, W.M., Nemani, R., Running, S.W., 2005. A generalized, bioclimatic index to predict foliar phenology in response to climate. *Glob. Change Biol.* 11 (4), 619–632.
- Jones, M.O., Jones, L.A., Kimball, J.S., McDonald, K.C., 2011. Satellite passive microwave remote sensing for monitoring global land surface phenology. *Remote Sens. Environ.* 115 (4), 1102–1114.
- Justice, C.O., Townshend, J.R.G., Holben, B.N., Tucker, C.J., 1985. Analysis of the phenology of global vegetation using meteorological satellite data. *Int. J. Remote Sens.* 6 (8), 1271–1318.
- Keenan, T.F., et al., 2014. Net carbon uptake has increased through warming-induced changes in temperate forest phenology. *Nat. Climate Change* 4, 598–604.
- Klosterman, S.T., et al., 2014. Evaluating remote sensing of deciduous forest phenology at multiple spatial scales using PhenoCam imagery. *Biogeosciences* 11 (16), 4305–4320.
- Liang, L., Schwartz, M.D., Fei, S.L., 2011. Validating satellite phenology through intensive ground observation and landscape scaling in a mixed seasonal forest. *Remote Sens. Environ.* 115 (1), 143–157.
- Liu, L.L., et al., 2015. Evaluating the potential of MODIS satellite data to track temporal dynamics of autumn phenology in a temperate mixed forest. *Remote Sens. Environ.* 160, 156–165.
- Lu, X.L., Liu, R.G., Liu, J.Y., Liang, S.L., 2007. Removal of noise by wavelet method to generate high quality temporal data of terrestrial MODIS products. *Photogramm. Eng. Remote Sens.* 73 (10), 1129–1139.
- Penuelas, J., Rutishauser, T., Filella, I., 2009. Phenology feedbacks on climate change. *Science* 324 (5929), 887–888.
- Piao, S.L., Fang, J.Y., Zhou, L.M., Ciais, P., Zhu, B., 2006. Variations in satellite-derived phenology in China's temperate vegetation. *Glob. Change Biol.* 12 (4), 672–685.
- Piao, S.L., et al., 2008. Net carbon dioxide losses of northern ecosystems in response to autumn warming. *Nature* 451 (7174), 49–U3.
- Reed, B.C., et al., 1994. Measuring phenological variability from satellite imagery. *J. Veg. Sci.* 5 (5), 703–714.
- Reed, B.C., Schwartz, M.D., Xiao, X., 2009. Remote sensing phenology. In: Noormets, A. (Ed.), *Phenology of Ecosystem Processes*. Springer, New York.
- Richardson, A.D., et al., 2010. Influence of spring and autumn phenological transitions on forest ecosystem productivity. *Philos. Trans. R. Soc. B-Biol. Sci.* 365 (1555), 3227–3246.
- Richardson, A.D., et al., 2013a. Climate change, phenology, and phenological control of vegetation feedbacks to the climate system. *Agric. Forest Meteorol.* 169, 156–173.
- Richardson, A.D., Klosterman, S., Toomey, M., 2013b. Near-surface sensor-derived phenology. In: Schwartz, M.D. (Ed.), *Phenology: An Integrative Environmental Science*. Springer, Dordrecht.
- Schwartz, M.D., 1999. Advancing to full bloom: planning phenological research for the 21st century. *Int. J. Biometeorol.* 42 (3), 113–118.
- Thompson, J.A., Paull, D.J., Lees, B.G., 2015. Using phase-spaces to characterize land surface phenology in a seasonally snow-covered landscape. *Remote Sens. Environ.* 166, 178–190.
- Townsend, P.A., et al., 2012. A general Landsat model to predict canopy defoliation in broadleaf deciduous forests. *Remote Sens. Environ.* 119, 255–265.
- Vermote, E.F., Kotchenova, S.Y., Ray, J.P., 2011. MODIS Surface Reflectance User's Guide. <http://modis-sr.ltdri.org/guide/MOD09.UserGuide.v1.3.pdf>.
- Walther, G.R., et al., 2002. Ecological responses to recent climate change. *Nature* 416 (6879), 389–395.
- White, M.A., Thornton, P.E., Running, S.W., 1997. A continental phenology model for monitoring vegetation responses to interannual climatic variability. *Glob. Biogeochem. Cycles* 11 (2), 217–234.
- Wu, C.Y., Gonsamo, A., Gough, C.M., Chen, J.M., Xu, S.G., 2014. Modeling growing season phenology in North American forests using seasonal mean vegetation indices from MODIS. *Remote Sens. Environ.* 147, 79–88.
- Xiao, X.M., Boles, S., Liu, J.Y., Zhuang, D.F., Liu, M.L., 2002. Characterization of forest types in Northeastern China, using multi-temporal SPOT-4 VEGETATION sensor data. *Remote Sens. Environ.* 82 (2–3), 335–348.
- Xiao, X.M., Zhang, J.H., Yan, H.M., Wu, W.X., Biradar, C., 2009. Land surface phenology: convergence of satellite and CO₂ Eddy Flux observations. In: Noormets, A. (Ed.), *Phenology of Ecosystem Processes*. Springer, New York.
- Yang, X., Tang, J., Mustard, J.F., 2014a. Beyond leaf color: comparing camera-based phenological metrics with leaf biochemical biophysical, and spectral properties throughout the growing season of a temperate deciduous forest. *J. Geophys. Res.-Biogeosci.* 119, 181–191.

- Yang, Y.T., Guan, H.D., Shen, M.G., Liang, W., Jiang, L., 2014b. [Changes in autumn vegetation dormancy onset date and the climate controls across temperate ecosystems in China from 1982 to 2010](#). *Glob. Change Biol.* 21 (2), 652–665.
- Zhang, X.Y., Goldberg, M.D., 2011. [Monitoring fall foliage coloration dynamics using time-series satellite data](#). *Remote Sens. Environ.* 115 (2), 382–391.
- Zhang, X.Y., et al., 2003. [Monitoring vegetation phenology using MODIS](#). *Remote Sens. Environ.* 84 (3), 471–475.
- Zhang, X.Y., Friedl, M.A., Tan, B., Goldberg, M.D., Yu, Y., 2012. [Long-term detection of global vegetation phenology from satellite instruments](#). In: Zhang, X.Y. (Ed.), *Phenology and Climate Change*. InTech.